Journal of Molecular Structure 1006 (2011) 678–683

Contents lists available at SciVerse ScienceDirect

Journal of Molecular Structure

journal homepage: www.elsevier.com/locate/molstruc

NMR crystallography of 2-acylamino-6-[1*H*]-pyridones: Solid-state NMR, GIPAW computational, and single crystal X-ray diffraction studies

Borys Ośmiałowski [a,*], Erkki Kolehmainen [b], Satu Ikonen [b], Kari Ahonen [b], Miika Löfman [b]

[a] Faculty of Chemical Technology and Engineering, University of Technology and Life Sciences, Seminaryjna 3, PL-85-326 Bydgoszcz, Poland
[b] Department of Chemistry, P.O. Box 35, FI-40014 University of Jyväskylä, Finland

ARTICLE INFO

Article history:
Received 16 August 2011
Received in revised form 17 October 2011
Accepted 17 October 2011
Available online 23 October 2011

Keywords:
Hydrogen bonding
X-ray diffraction
NMR crystallography
GIPAW calculations

ABSTRACT

2-Acylamino-6-[1*H*]-pyridones [acyl = RCO, where R = methyl (**1**), ethyl (**2**), *iso*-propyl (**3**), *tert*-butyl (**4**), and 1-adamantyl (**5**)] have been synthesized and characterized by NMR spectroscopy. From three congeners, **2**, **3** and **5**, also single crystal X-ray structures have been solved. For these derivatives GIPAW calculations acts as a "bridge" between solid-state NMR data and calculated chemical shifts based on X-ray determined geometry. In crystals all three compounds exist as pyridone tautomers possessing similar six-membered ring structure stabilized by intramolecular C=O···HN hydrogen bond. Theoretical GIPAW calculated and experimental ^{13}C and ^{15}N CPMAS NMR shifts are in excellent agreement with each other.

1. Introduction

Double hydrogen bonding is known to be strong enough to stabilize dimers. As a classical example, 2-[1*H*]-pyridone/2-hydroxypyridine (Fig. 1) was suggested as being the most stable double hydrogen-bonded dimer [1] although secondary interactions [2,3] may support even more stable dimeric structure of related compounds [4].

2-Acylaminopyridines (Fig. 2b) also can form two hydrogen bonds. If a large alkyl group is a part of acyl moiety or a methyl locates at C-6 crystal structure of these compounds are ribbon-like stabilized by NH···O hydrogen bonds [5]. We have shown that the steric hindrance [6] and electronic repulsion [7] may effectively influence the association of triple hydrogen bonded associates in solution of 2,6-bis(acylamino)-pyridines (Fig. 2c).

The topology 2-acylamino-6-[1*H*]-pyridone (Fig. 2a) can be thought as a combination of those of 2-[1*H*]-pyridone and 2-acylaminopyridine, where an ADD (acceptor–donor–donor) hydrogen bonding motif is present in the pyridone tautomer as in guanine [2]. 2-Acylamino-6-[1*H*]-pyridinones can also form intramolecular hydrogen-bond acting as a configurational lock similar to those in 2-phenacylpyridines or ureas [8–12] (Scheme 1). The 1,3-proton shift (tautomerism) may also occur in these molecules.

The difference between 2-phenacylpyridines and urea derivatives (Scheme 1) is that in latter case the proton shift (tautomerism) does not take place. The urea derivatives in its unfolded form are able to form heterocomplexes stabilized by three intermolecular hydrogen bonds [13–22]. In some other urea derivatives the intramolecular hydrogen-bonding restricts the rotation about single bonds (folding/configurational lock), which is reflected in higher association/dimerization constants for example in ureidopyrimidine derivatives [23–25] (Fig. 3).

If the intramolecular hydrogen bonding is strong enough it may lead to the stabilization of the "locked form" both in solution and solid state [9–11,26,27]. Since 2-acylamino-6-[1*H*]-pyridones are used in asymmetric organocatalysis [15] understanding of their structure and intermolecular interactions is important. The GIPAW calculations, solid-state NMR and XRD were used together in studies on molecular structure [28–36]. The GIPAW technique was also used in studies based on ^{1}H solid-state NMR experiments [29,32,37].

The aims of this study are (a) to clarify the tautomeric preferences of 2-acylamino-6-[1*H*]-pyridones both in solution and in solid state; (b) to compare experimental and calculated NMR parameters; (c) to study what kind of intermolecular interactions are preferred; and (d) to find out what is the influence of steric crowding on structure of studied compounds.

2. Experimental methods

2.1. Syntheses

The compounds **1**–**5** were synthesized allowing acid chlorides (Aldrich) to react with 6-amino-2-[1*H*]-pyridone in boiling pyridine under magnetic stirring. After 6 h reaction period, pyridine

* Corresponding author. Fax: +48 52 3749005.
E-mail address: borys.osmialowski@utp.edu.pl (B. Ośmiałowski).

0022-2860/$ - see front matter © 2011 Elsevier B.V. All rights reserved.
doi:10.1016/j.molstruc.2011.10.034

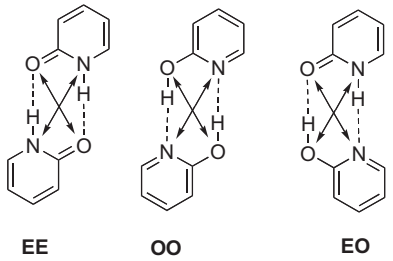

Fig. 1. Dimers of 2-[1*H*]-pyridone (**E**) and 2-hydroxypyridine (**O**).

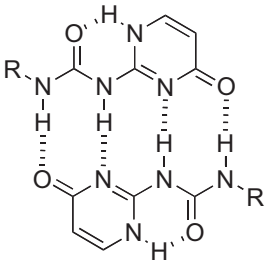

Fig. 3. Dimerization of ureidopyrimidine derivatives.

was removed in *vacuo*. The crude product was washed with water and cold ethanol. Recrystallization from ethanol gave the desired products with yields varying 75–80%. The melting points were determined with Büchi apparatus (K-565) using the 2 °C/min gradient. The compound **5** was not pure enough after recrystallization. It was purified by column chromatography on silica using hexane/ethyl acetate 10:1 (v/v) as eluent. The ^{13}C NMR spectrum of **1** contains signals (values in italics) that come from another form (dimer) of compound **1**. Dimerization is confirmed by dilution experiments, but homo- and heteroassociation of these compounds will be a subject of separate paper.

1: Mp 212.2–214.4 °C (lit. 212–215 °C[38]), ^{1}H NMR ($CDCl_3$) δ: 11.05 (bs, 1H, H1), 7.61 (dd, $^3J_{H,H}$ = 8.0 Hz, 1H, H4), 6.93 (d, $^3J_{H,H}$ = 8.0 Hz, 1H, H5), 6.39 (d, $^3J_{H,H}$ = 8.0 Hz, 1H, H3), 2.29 (s, 3H, CH_3); ^{13}C NMR 172.51 (C9), *169.23* (C9′), 161.06 (C6), *154.78* (C6′), *149.97* (C2′), *145.53* (C4′), 144.35 (C2), 142.60 (C4), *112.43* (C5′), 110.44 (C5), *109.38* (C3′), 97.75 (C3), *24.87* (CH_3'), 24.52 (CH_3). Anal. Calcd.: C 55.26, H 5.30, N 18.41. Found: C 55.28, H 5.25, N 18.37.

2: Mp 203.8–208.2 °C, ^{1}H NMR ($CDCl_3$) δ: 11.49 (bs, 1H, H1), 9.55 (bs, 1H, H8), 7.45 (dd, $^3J_{H,H}$ = 8.0 Hz, 1H, H4), 6.68 (d, $^3J_{H,H}$ = 8.0 Hz, 1H, H5), 6.20 (d, $^3J_{H,H}$ = 8.0 Hz, 1H, H3), 2.44 (q, 2H, CH_2), 1.24 (t, 3H, CH_3); ^{13}C NMR 173.34 (C9), 162.42 (C6), 143.58 (C2), 143.40 (C4), 111.77 (C5), 95.14 (C3), 30.81 (CH_2), 9.13 (CH_3). Anal. Calcd.: C 57.82, H 6.07, N 16.86. Found: C 57.86, H 6.01, N 16.81.

3: Mp 158.0–161.0 °C, ^{1}H NMR ($CDCl_3$) δ: 11.84 (bs, 1H, H1), 10.54 (bs, 1H, H8), 7.46 (dd, $^3J_{H,H}$ = 8.0 Hz, 1H, H4), 6.81 (d, $^3J_{H,H}$ = 8.0 Hz, 1H, H5), 6.15 (d, $^3J_{H,H}$ = 8.0 Hz, 1H, H3), 2.61 (septet, $^3J_{H,H}$ = 7.0 Hz, 1H, CH), 1.23 (d, $^3J_{H,H}$ = 7.0 Hz, 6H, CH_3); ^{13}C NMR 177.23 (C9), 162.53 (C6), 144.04 (C2), 143.82 (C4), 111.43 (C5), 95.40 (C3), 36.66 (methine), 19.18 (CH_3). Anal. Calcd.: C 59.99, H 6.71, N 15.55. Found: C 59.94, H 6.67, N 15.49.

4: Mp 213.5–216.0 °C, ^{1}H NMR ($CDCl_3$) δ: 12.07 (bs, 1H, H1), 9.69 (bs, 1H, H8), 7.43 (dd, $^3J_{H,H}$ = 8.0 Hz, 1H, H4), 6.96 (d, $^3J_{H,H}$ = 8.0 Hz, 1H, H5), 6.16 (d, $^3J_{H,H}$ = 8.0 Hz, 1H, H3), 1.30 (s, 9H, CH_3); ^{13}C NMR 178.42 (C9), 162.72 (C6), 143.81 (C2), 143.79 (C4), 111.65 (C5), 95.86 (C3), 40.29 (quaternary C), 27.16 (CH_3).

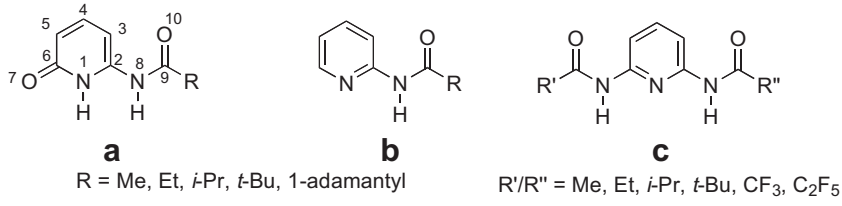

Fig. 2. The structures of studied compounds (a), 2-acylaminopyridines (b) and 2,6-bis(acylamino)pyridines (c).

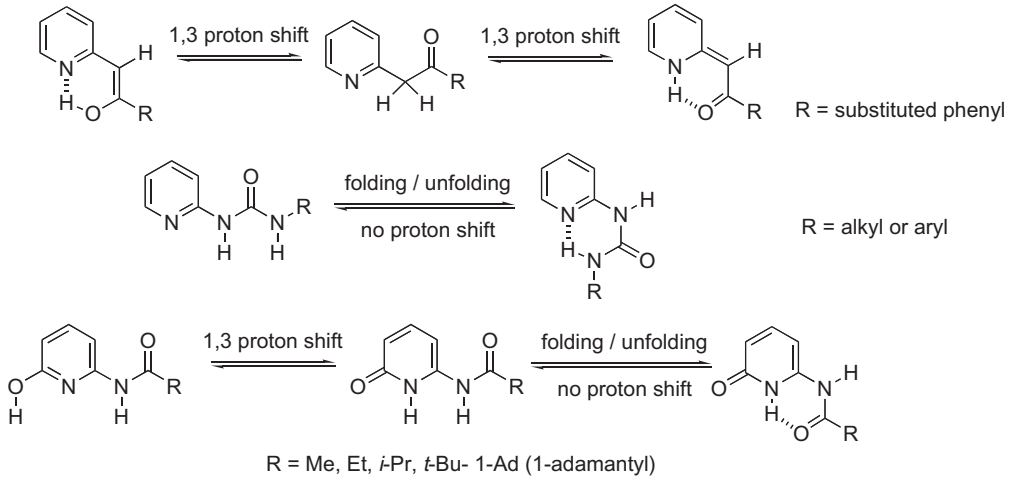

Scheme 1. The configurational lock in enolimine/enaminone form of 2-phenacylpyridines, urea derivative and possible forms in subjected compounds.

Anal. Calcd.: C 61.84, H 7.27, N 14.42. Found: C 61.80, H 7.30, N 14.37.

5: Mp 250.2–254.0 °C, ^{1}H NMR ($CDCl_3$) δ: 12.04 (bs, 1H, H1), 8.60 (bs, 1H, H8), 7.42 (dd, $^3J_{H,H}$ = 7.6 Hz, 1H, H4), 6.62 (d, $^3J_{H,H}$ = 7.6 Hz, 1H, H5), 6.23 (d, $^3J_{H,H}$ = 7.8 Hz, 1H, H3); ^{13}C NMR 177.67 (C9), 162.63 (C6), 143.85 (C2), 143.14 (C4), 112.01 (C5), 95.32 (C3), 42.13 (substituent's quaternary carbon), 38.78 (CH_2), 36.31 (CH), 28.00 (CH_2). Anal. Calcd.: C 70.56, H 7.40, N 10.29. Found: C 70.53, H 7.44, N 10.24.

2.2. Spectroscopy

The liquid state ^{1}H and ^{13}C NMR and 2 D PFG ^{1}H,^{1}H COSY, PFG ^{1}H,^{13}C HMQC and PFG ^{1}H,X (X = ^{13}C and^{15}N) HMBC spectra were recorded with a Bruker Avance DRX 500 NMR spectrometer equipped with an inverse detection probehead and a *z*-gradient accessory for structure verification and chemical shift assignments. The chemical shifts are referenced to internal TMS (δ = 0.00 ppm). ^{13}C and^{15}N CPMAS NMR spectra were recorded with a Bruker Avance 400 spectrometer equipped with 4 mm dual CPMAS probehead. The chemicals shifts are referenced to the signals of the glycine standard measured prior to every sample. Spectrometer was working at 100.62 MHz (for ^{13}C) and 40.55 MHz (for ^{15}N). The samples were spun at 10 kHz rate in 4 mm zirconia rotors. Other NMR acquisition and processing parameters can be found in our previous publications [7,39].

2.3. X-ray crystallography

Single crystals of 2-amino-6-[1*H*]-pyridone, **2**, **3** and **5** suitable for X-ray diffraction experiments were grown in ethanol at ambient temperature. The obtained single crystals were mounted with perfluoro polyether oil on a Nylon loop sample holder. Data were collected at 123(2) K on a Nonius KappaCCD diffractometer with ApexII using graphite monochromated Mo Kα radiation. COLLECT [40] data collection software was utilized for data collection and data were processed with DENZO-SMN [41]. The structures were solved by direct methods (SIR2002 [42] or SHELXS-97 [43]) and refined anisotropically by full matrix least squares on F^2 values utilizing SHELXL-97 [43]. Hydrogen atoms bound to carbons were positioned according to the expected geometry and were refined only isotropically riding on the parent atom. Hydrogen atoms bound to nitrogen were located from the electron density map. Figures were drawn with Ortep-3 [44] for Windows and Mercury [45]. Crystal data and parameters with the ORTEP plots for the compounds can be found in the Supporting Information.

2.4. GIPAW calculations

The geometry optimizations and the NMR spectroscopic calculations were performed with the DFT-based CASTEP and NMR-CASTEP programs [46–49]. The positions of the hydrogen atoms were optimized with the BFGS method applying "ultrasoft" pseudopotentials, keeping the heavy atoms and the lattice volume fixed. C and N atomic forces were below 1 eV/Å after optimization. The gauge-including projector-augmented wave (GIPAW) procedure was used for the prediction of the magnetic resonance parameters [47]. The plane wave DFT with generalized gradient approximation (GGA) Perdew–Burke–Ernzerhof exchange–correlation functional (PBE) was used with "on-the-fly" generated pseudopotentials in NMR calculations, sampling *k*-points with 1 × 5 × 3 or 2 × 3 × 2 Monkhorst–Pack grids at an energy cutoff level of 440 eV or 550 eV. The chemical shielding tensors were calculated for ^{13}C and ^{15}N nuclei for the geometry optimized structures and the ones derived from the X-ray crystal structures of **2** and **3**. The chemical shifts were calculated from absolute shielding values with the following formula δ(sample) = σ(sample) − σ(*glycine*) + δ(glycine). Proton optimized structure of glycine was used in these calculations. In ^{13}C CPMAS we used glycine C=O at 176.03 ppm from int. TMS (0.00 ppm) as a reference and in ^{15}N CPMAS glycine NH_2 at −347.4 ppm (from ext. CH_3NO_2) as a reference. Glycine sample was measured with number of scans = 4 before each sample.

Table 1
^{13}C and ^{15}N CP MAS NMR chemical shifts of **2**, **3** and **5** at 296 K.

	2[a]	**3**	**5**
C2	145.8	145.3	146.3
C3	93.5	94.9	92.3
C4	145.1	142.4	142.9
C5	111.1	111.0	112.4
	112.1		
C6	162.5	160.3	161.2
C9	175.2	179.1	181.7
	174.9		
Other	28.0	35.4	42.3
	7.9	21.9	39.0
	7.5	18.6	36.8
			28.1
N1	−221.2	−223.1	−222.3
	−222.7		
N8	−248.2	−250.2	−255.9
	−250.4		

[a] Two molecules are present in asymmetric unit.

Table 2
Selected torsion angles (°) in the molecules **2**, **3** and **5** in solid state.

	2	**3**	**5**
N(1)—C(2)—N(8)—C(9)	13.3(2)/−1.45(2)	1.8(2)	−0.3(2)
C(2)—N(8)—C(9)—O(10)	9.4(2)/−4.8(2)	1.8(3)	−2.0(2)
C(2)—C(8)—C(9)—R	−168.0(1)/174.5(1)	−175.5(1)	178.4(1)

Table 3
Hydrogen bonding geometries (Å, °) in the crystals of 2-amino-6-[1*H*]-pyridone and **2**, **3** and **5**.

	D(H···A)	*d*(D···A)	<(DHA)
2-amino-6-[1H]-pyridone			
N(1)···O(7)#1	1.835(19)	2.7374(15)	163.4(16)
N(8)···O(7)#2	1.93(2)	2.8403(16)	177(2)
N(8)···O(7)#1	2.31(2)	3.0504(16)	139.0(16)
2			
N(1A)···O(10A)	2.030(16)	2.6794(14)	130.9(13)
N(1B)···O(10B)	1.981(18)	2.6742(13)	131.3(14)
N(1B)···O(7B)	2.527(18)	3.1136(14)	122.4(14)
N(8B)···O(7A)#3	1.854(16)	2.7579(13)	175.9(15)
N(8A)···O(7B)#4	1.854(19)	2.7370(13)	167.0(17)
3			
N(1)···O(10)	1.96(2)	2.6633(17)	135.5(18)
N(8)···O(7)#5	1.81(2)	2.6881(17)	167(2)
5			
N(1)···O(10)	1.864(16)	2.6127(14)	137.8(15)
N(8)···O(7)#6	1.938(18)	2.8294(14)	170.0(15)

#1 $x-1/2, -y-1/2, -z-1$; #2 $-x-1/2, -y-1, z+1/2$; #3 $-x+1, y-1/2, -z+3/2$; #4 $-x, -y+1, -z+1$; #5 $-x+3/2, y-1, z-1/2$; #6 $-x+1, y+1/2, -z-1/2$.

3. Results and discussion

3.1. NMR spectroscopy

^{13}C and ^{15}N NMR spectra of **2**, **3** and **5** were recorded in the solid state. Table 1 collects selected data. For compounds **1** and **4** the

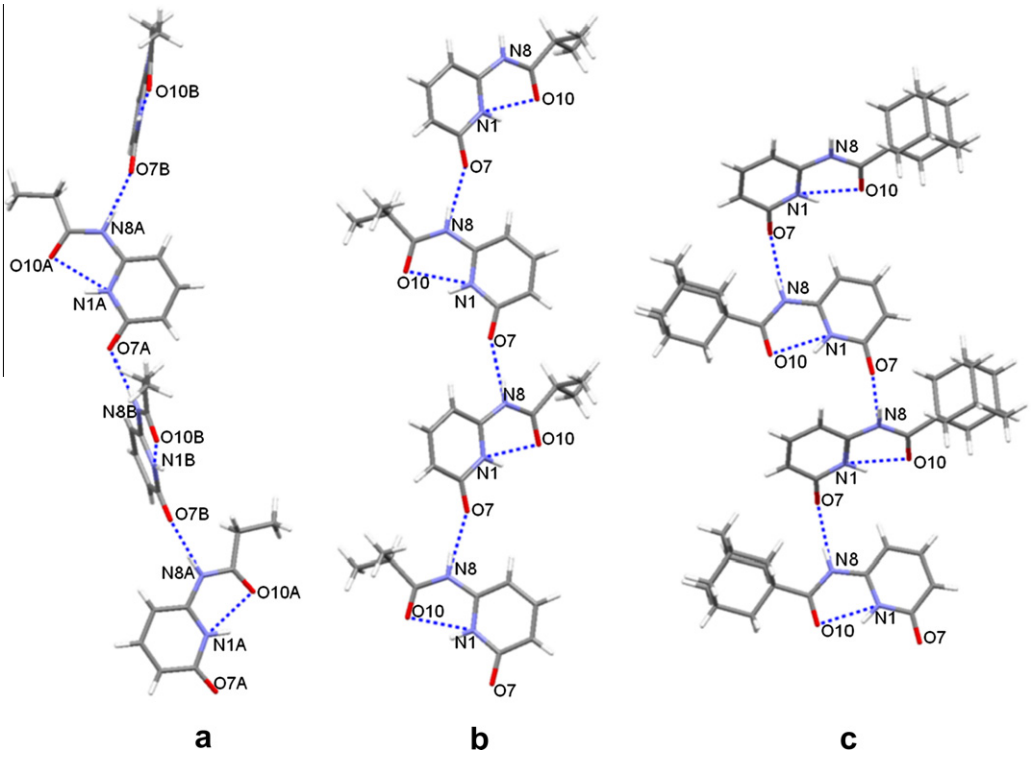

Fig. 4. Hydrogen bonding chains in crystals of **2**, **3** and **5**.

Table 4
^{13}C NMR chemical shifts of experiment and calculated results from crystal structure (**2a**), after optimized hydrogen locations (**2b**), and **2b** with fixed N1H1···O10 hydrogen bond (**2c**).

Atom	Exp.	2a	2b	2c
C2	145.8	143.5	145.7	145.0
C2′	145.8	143.7	146.0	145.3
C3	93.6	87.5	95.6	94.9
C3′	93.6	87.7	95.6	94.9
C4	145.1	142.9	146.5	146.3
C4′	145.1	143.1	146.6	146.4
C5	111.2	108.3	113.2	114.0
C5′	112.1	110.2	114.8	115.5
C6	162.5	161.3	160.1	160.1
C6′	162.5	161.8	160.3	160.5
C9	174.9	174.7	176.2	175.9
C9′	175.2	175.4	176.8	176.6
CH_2	27.4	10.2	25.7	25.5
CH_2	28.0	11.1	26.9	26.6
CH_3	7.5	−19.7	3.9	3.7
CH_3'	7.9	−19.2	4.7	4.6
N1	−222.7	−237.3	−220.6	−223.0
N1′	−221.2	−236.0	−223.2	−220.4
N8	−250.4	−255.4	−240.9	−251.4
N8′	−248.2	−253.5	−238.7	−249.7

amounts of good quality crystals were not sufficient to record $^{13}C/^{15}N$ CP MAS NMR spectra and the quality of obtained crystals was too low for solving their solid-state structure with the use of XRD. ^{1}H and ^{13}C NMR spectra of **1–5** in $CDCl_3$ solutions are collected in Supporting information.

The liquid ($CDCl_3$) state chemical shifts (spectra in SI) show clearly that in **1–5** intramolecular hydrogen bond is present (deshielding of H1 signal due to interaction with O10). The ^{13}C and ^{15}N NMR chemical shifts in $CDCl_3$ solution and in solid state are comparable. This gives a reason to conclude that in the non-polar solvent and in the solid-state, the structures of studied molecules are similar.

Table 5
Experimental and calculated NMR chemical shifts from crystal structure (**3a**), after optimized hydrogen locations (**3b**), and with fixed N1H1···O10 hydrogen bond length (**3c**).

Atom	Exp.	3a	3b	3c
C2	145.3	144.4	146.8	146.1
C3	94.9	90.0	97.2	96.6
C4	142.4	139.7	143.2	142.9
C5	111.0	107.4	112.5	113.1
C6	160.3	158.2	156.6	157.0
C9	179.1	180.7	180.3	180.0
Methine CH	35.4	24.7	35.1	34.7
CH_3'	21.9	−3.9	20.7	20.7
CH_3	18.6	−8.7	16.4	16.2
N1	−223.1	−239.5	−222.5	−222.8
N8	−250.2	−257.2	−240.7	−252.1

3.2. X-ray crystallography

In order to get insight into the molecular structure and crystal packing of these compounds in solid state they were crystallized from ethanol at ambient temperature. Single crystals suitable for X-ray diffraction were obtained from the starting material, 2-amino-6-[1*H*]-pyridone, and from conjugates **2**, **3** and **5**. Unfortunately compounds **1** and **4** did not give crystals of good enough quality to be solved by XRD. Crystal data and refinement parameters are listed in Table S1 in the Supporting information. 2-Amino-6-[1*H*]-pyridone was crystallized in orthorhombic space group $P2_12_12_1$. Compounds **2** and **5** were both crystallized in monoclinic space group $P2_1/c$, but whereas **5** had only one, **2** had two crystallographically independent molecules in the asymmetric unit. Compound **3** was crystallized in orthorhombic space group $Pca2_1$. The most important geometrical parameters describing the molecular structure of 2-amino-6-[1*H*]-pyridone and **2**, **3** and **5** in solid state are collected in Tables 2 and 3. Ortep-plots of the

Table 6
The effect of the hydrogen bond length on the principal shielding tensor δ_{22}, which is the most sensitive to hydrogen bonding [50].

	2a	2b	2c	3a	3b	3c
N1H 1···O10 (Å)	1.85/1.85	1.70/1.70	1.80/1.80	1.82	1.65	1.76
δ_{22}	151.8/ 152.7	126.1/ 124.8	143.7/ 142.9	153.4	124.6	143.0

molecular structures of the studied compounds are given in the Supporting information (Fig. S1). In all of the studied conjugates the amide side chain verges a perfect ziczac illustrated by the torsion angle C(2)—N(8)—C(9)—R. The two molecules in the asymmetric unit of **2** differ slightly by the conformation of their side chains as illustrated by the difference in the absolute value of the torsion angle C(2)—N(8)—C(9)—R (168.05(11)° for molecule A and 174.49(12)° for molecule B, respectively). Further, in all of the studied structures the amide carbonyl is *cis* to ring nitrogen, as described by the torsion angle N(1)—C(2)—N(8)—C(9) and this orientation is stabilized by an intramolecular hydrogen bond (N(1)···O(10)) with a hydrogen bond motif $R_1^1(6)$.

In all of these crystals, hydrogen bonding plays important role in the crystal packing. Besides of the hydrogen bonding interactions, the interactions between the heterocyclic π-systems may contribute to the packing in the crystals of **5** and **3**. Hydrogen bonding geometries in the studied crystals are collected in Table 3 and illustrated in Fig. 4. In the crystals of 2-amino-6-[1*H*]-pyridone the hydrogen bonding network (Fig. S2) is constructed by hydrogen bonded chain $C_1^1(5)$ *via* N(1)···O(7) ($x-1/2, -y-1/2, -z-1$; 2.74 Å, 163.4°) hydrogen bonds running along *a*-axis and further stabilized by N(8)···O(7) ($x-1/2, -y-1/2, -z-1$; 3.05 Å, 139.0°) hydrogen bonds and another hydrogen bonded chain $C_1^1(7)$ *via* N(8)···O(7) ($-x-1/2, -y-1, z+1/2$; 2.84 Å, 177°) hydrogen bonds running along *c*-axis.

In the crystals of **2** hydrogen bonded chains $C_2^2(12)$ where the molecules A and B alternate are formed *via* N(8A)···O(7B) ($-x, -y+1, -z+1$; 2.74 Å, 167°) and N(8B)···O(7A) ($-x+1, y-1/2, -z+3/2$; 2.76 Å, 175.9°) interactions. There is also a weak hydrogen bonding interaction between the adjacent chains through N(1B)···O(7B) (3.11 Å, 122.4°) hydrogen bond. In the crystals of **3** again hydrogen bonded chain $C_1^1(6)$ *via* N(8)···O(7) ($-x+3/2, y-1, z-1/2$; 2.69 Å, 167.0°) hydrogen bond is formed. In these crystals the parallel chains are piled on top of each other with the rings stacked offset with 4.97 Å centroid to centroid distance. Similarly in the crystals of **5** hydrogen bonded chains $C_1^1(6)$ running along *b*-axes are formed through N(8)···O(7) ($-x+1, y+1/2, -z-1/2$; 2.83 Å, 170°) hydrogen bond. Further, the adjacent antiparallel chains are assembled in such way that the heterocyclic rings are stacked offset with centroid to centroid distance of 4.86 Å.

This is worth noting that the intramolecular hydrogen bond length decreases when the substituent R become larger (the N(1)···O(10) distance, Table 3). The opposite is realized for N–H···O angle (<(DHA), Table 3).

3.3. GIPAW calculations

The GIPAW calculations were based on X-ray structures (Fig. 4), and structures where hydrogen atom positions were optimized. NMR calculations were performed with cut-off energy level 440 eV, resulting comparable results in the case of **2**, where as **3** resulted 10 ppm underestimation of the absolute shielding of pyridine nitrogen and cut-off energy level 550 eV was used for chemical shielding calculations of **3**. In the case of **2c** and **3c**, the hydrogen bond length of the amide nitrogen donor and ring carbonyl acceptor was fixed to 1.80 Å and 1.76 Å, respectively (Tables 4–6), in order to gain higher correspondence of chemical shielding values of amide nitrogen's. The selected hydrogen bond lengths were based on linear correlation of shielding values of non-optimized structures and proton optimized structures since the experimental value was between them.

4. Conclusions

Single crystal X-ray structural data of three 2-acylamino-6-[1*H*]-pyridones shows that all of them exist as pyridone tautomers stabilized by intramolecular NH···O=C hydrogen-bonded six-membered ring structure. Further, the molecules arrange in hydrogen-bonded chains, which are packed either with or without base stacking interactions. The hydrogen bonding geometries in these chains are quite similar despite of different substituent and the difference in the side chain seems to affect mostly to the packing of these chains in respect with each other. No dimer formation *via* hydrogen bonding was observed in the single crystals. The intramolecular hydrogen bonding is to some extent related to the size of the substituent. Comparison of liquid and solid-state ^{13}C and ^{15}N NMR data suggests that the preferred tautomer is pyridone form in both cases. Theoretical GIPAW calculated and experimental ^{13}C CPMAS NMR chemical shifts are in agreement with each other after optimization of the hydrogen positions derived from the X-ray structure. In addition, the position of hydrogen in the hydrogen bond is needed to manually optimized using linear correlation of shielding values of ^{15}N in non-optimized and proton optimized structures in order to gain high correspondence between calculated and experimental ^{15}N NMR chemical shift values.

Acknowledgements

Financial support from the Polish Ministry of Science and Higher Education (Grant No. N N204 174138) is gratefully acknowledged. The authors acknowledge CSC – IT Center for Science Ltd. for the allocation of computational resources for CASTEP calculations. K.A. is grateful to Academy of Finland for financial support (Project No. 127006). Academy Researcher Elina Sievänen and Academy of Finland (Project No. 119616 and 255648) are thanked for financial support for M.L. CCDC 839166–839169 contains the supplementary crystallographic data for this paper. These data can be obtained free of charge *via* external link http://www.ccdc.cam.ac.uk/conts/retrieving.html (or from the Cambridge Crystallographic Data Centre, 12, Union Road, Cambridge CB2 1EZ, UK; fax: +44 1223 336033).

Appendix A. Supplementary material

Supplementary data associated with this article can be found, in the online version, at doi:10.1016/j.molstruc.2011.10.034.

References

[1] A. Müller, M. Losada, S. Leutwyler, J. Phys. Chem. A 108 (2004) 157–165.
[2] W.L. Jorgensen, J. Pranata, J. Am. Chem. Soc. 112 (1990) 2008–2010.
[3] J. Pranata, S.G. Wierschke, W.L. Jorgensen, J. Am. Chem. Soc. 113 (1991) 2810–2819.
[4] B. Ośmiałowski, R. Dobosz, J. Mol. Model. (in print).
[5] B. Ośmiałowski, E. Kolehmainen, R. Dobosz, R. Gawinecki, R. Kauppinen, A. Valkonen, J. Koivukorpi, K. Rissanen, J. Phys. Chem. A 114 (2010) 10421–10426.
[6] B. Ośmiałowski, E. Kolehmainen, R. Gawinecki, R. Dobosz, R. Kauppinen, J. Phys. Chem. A 114 (2010) 12881–12887.
[7] B. Ośmiałowski, E. Kolehmainen, R. Gawinecki, R. Kauppinen, J. Koivukorpi, A. Valkonen, Struct. Chem. 21 (2010) 1061–1067.
[8] L. Xing, C. Wiegert, A. Petitjean, J. Org. Chem. 74 (2009) 9513–9516.
[9] E. Kolehmainen, B. Ośmiałowski, T.M. Krygowski, R. Kauppinen, M. Nissinen, R. Gawinecki, J. Chem. Soc., Perkin Trans. 2 (2000) 1259–1266.

[10] E. Kolehmainen, B. Ośmiałowski, M. Nissinen, R. Kauppinen, R. Gawinecki, J. Chem. Soc., Perkin Trans. 2 (2000) 2185–2191.
[11] B. Ośmiałowski, E. Kolehmainen, M. Nissinen, T.M. Krygowski, R. Gawinecki, J. Org. Chem. 67 (2002) 3339–3345.
[12] R. Gawinecki, E. Kolehmainen, H. Loghmani-Khouzani, B. Osmialowski, T. Lovasz, P. Rosa, Eur. J. Org. Chem. 2006 (2006) 2817–2824.
[13] C.-H. Chien, J. Org. Chem. 69 (2004) 1866–1871.
[14] K. Sugita, D. Sawada, M. Sodeoka, H. Sasai, M. Shibasaki, Chem. Pharm. Bull. (Tokyo) 44 (1996) 463–465.
[15] M.L. Clarke, J.A. Fuentes, Angew. Chem. Int. Ed. 46 (2007) 930–933.
[16] Y. Hisamatsu, N. Shirai, S.-I. Ikeda, K. Odashima, Org. Lett. 12 (2010) 1776–1779.
[17] A. Gooch, A.M. McGhee, M.L. Pellizzaro, C.I. Lindsay, A.J. Wilson, Org. Lett. 13 (2011) 240–243.
[18] S. Brammer, U. Lüning, C. Kühl, Eur. J. Org. Chem. 2002 (2002) 4054–4062.
[19] T.F.A. de Greef, M.M.L. Nieuwenhuizen, P.J.M. Stals, C.F.C. Fitié, A.R.A. Palmans, R.P. Sijbesma, E.W. Meijer, Chem. Commun. (2008) 4306–4308.
[20] E.B. Berda, E.J. Foster, E.W. Meijer, Macromolecules 43 (2010) 1430–1437.
[21] D. Guo, R.P. Sijbesma, H. Zuilhof, Org. Lett. 6 (2004) 3667–3670.
[22] B.W.T. Gruijters, M.A.C. Broeren, F.L. van Delft, R.P. Sijbesma, P.H.H. Hermkens, F.P.J.T. Rutjes, Org. Lett. 8 (2006) 3163–3166.
[23] H. Sun, A.E. Kaifer, Org. Lett. 7 (2005) 3845–3848.
[24] A.T. ten Cate, H. Kooijman, A.L. Spek, R.P. Sijbesma, E.W. Meijer, J. Am. Chem. Soc. 126 (2004) 3801–3808.
[25] C. Schmuck, W. Wienand, Angew. Chem. Int. Ed. 40 (2001) 4363–4369.
[26] B. Ośmiałowski, E. Kolehmainen, R. Gawinecki, Chem. Eur. J. 9 (2003) 2710–2716.
[27] R. Gawinecki, A. Kuczek, E. Kolehmainen, B. Ośmiałowski, T.M. Krygowski, R. Kauppinen, J. Org. Chem. 72 (2007) 5598–5607.
[28] J.P. Bradley, S.P. Velaga, O.N. Antzutkin, S.P. Brown, Cryst. Growth Des. 11 (2011) 3463–3471.
[29] A.L. Webber, B. Elena, J.M. Griffin, J.R. Yates, T.N. Pham, F. Mauri, C.J. Pickard, A.M. Gil, R. Stein, A. Lesage, L. Emsley, S.P. Brown, Phys. Chem. Chem. Phys. 12 (2010) 6970–6983.
[30] R.K. Harris, P. Hodgkinson, V. Zorin, J.-N. Dumez, B. Elena-Herrmann, L. Emsley, E. Salager, R.S. Stein, Magn. Reson. Chem. 48 (2010) S103–S112.
[31] S. Cadars, A. Lesage, C.J. Pickard, P. Sautet, L. Emsley, J. Phys. Chem. A 113 (2009) 902–911.
[32] A.-C. Uldry, J.M. Griffin, J.R. Yates, M. Perez-Torralba, J. Am. Chem. Soc. 130 (2008) 945–954.
[33] R.K. Harris, P. Hodgkinson, C.J. Pickard, J.R. Yates, V. Zorin, Magn. Reson. Chem. 45 (2007) S174–S186.
[34] J.R. Yates, C.J. Pickard, F. Mauri, Phys. Rev. B 76 (2007) 024401.
[35] R.K. Harris, P.Y. Ghi, R.B. Hammond, C.Y. Ma, K.J. Roberts, J.R. Yates, C.J. Pickard, Magn. Reson. Chem. 44 (2006) 325–333.
[36] C. Gervais, R. Dupree, K.J. Pike, C. Bonhomme, M. Profeta, C.J. Pickard, F. Mauri, J. Phys. Chem. A 109 (2005) 6960–6969.
[37] J.R. Yates, T.N. Pham, C.J. Pickard, F. Mauri, A.M. Amado, A.M. Gil, S.P. Brown, J. Am. Chem. Soc. 127 (2005) 10216–10220.
[38] C.-D. Li, L.S. Rittmann, A.S. Tsiftsoglou, K.K. Bhargava, A.C. Sartorelli, J. Med. Chem. 21 (1978) 874–877.
[39] B. Ośmiałowski, E. Kolehmainen, E. Sievanen, R. Kauppinen, B. Behera, J. Mol. Struct. 931 (2009) 60–67.
[40] COLLECT, in: Bruker AXS, Inc., Madison, Wisconsin, USA, 2008.
[41] Z. Otwinowski, W. Minor, Methods in Enzymology, Macromolecular Crystallography, vol. 276, Academic Press, New York, 1997.
[42] M.C. Burla, M. Camalli, B. Carrozzini, G.L. Cascarano, C. Giacovazzo, G. Polidori, R. Spagna, J. Appl. Crystallogr. 36 (2003) 1103.
[43] G.M. Sheldrick, Acta Crystallog. A 64 (2008) 112–122.
[44] L.J. Farrugia, J. Appl. Crystallogr. 30 (1997) 565–566.
[45] C.F. Macrae, P.R. Edgington, P. McCabe, E. Pidcock, G.P. Shields, R. Taylor, M. Towler, J. van de Streek, J. Appl. Crystallogr. 39 (2006) 453–457.
[46] S.J. Clark, M.D. Segall, C.J. Pickard, P.J. Hasnip, M.J. Probert, K. Refson, M.C. Payne, Z. Kristallogr. 220 (2005) 567–570.
[47] C.J. Pickard, F. Mauri, Phys. Rev. B63 (2001) 245101–245113.
[48] J.R. Yates, C.J. Pickard, F. Mauri, Phys. Rev. B76 (2007) 024401–024411.
[49] M. Profeta, F. Mauri, C.J. Pickard, J. Am. Chem. Soc. 125 (2002) 541–548.
[50] Y. Wei, D.-K. Lee, A. Ramamoorthy, J. Am. Chem. Soc. 123 (2001) 6118–6126.